Containment-Based Multiple PCC Voltage Regulation Strategy for Communication Link and Sensor Faults

Meina Zhai 🆔, Qiuye Sun 🆔, *Senior Member, IEEE*, Rui Wang 🆔, and Huaguang Zhang 🆔, *Fellow, IEEE*

Abstract—The distributed AC microgrid (MG) voltage restoration problem has been extensively studied. Still, many existing secondary voltage control strategies neglect the co-regulation of the voltage at the point of common coupling (PCC) in the AC multi-MG system (MMS). When an MMS consists of sub-MGs connected in series, power flow between the sub-MGs is not possible if the PCC voltage regulation relies on traditional consensus control objectives. In addition, communication faults and sensor faults are inevitable in the MMS. Therefore, a resilient voltage regulation strategy based on containment control is proposed. First, the feedback linearization technique allows us to deal with the nonlinear distributed generation (DG) dynamics, where the PCC regulation problem of an AC MG is transformed into an output feedback tracking problem for a linear multi-agent system (MAS) containing nonlinear dynamics. This process is an indispensable pre-processing in control algorithm design. Moreover, considering the unavailability of full-state measurements and the potential faults present in the sensors, a novel follower observer is designed to handle communication faults. Based on this, a controller based on containment control is designed to achieve voltage regulation. In regulating multiple PCC voltages to a reasonable upper and lower limit, a voltage difference exists between sub-MGs to achieve power flow. In addition, the secondary control algorithm avoids using global information of directed communication network and fault boundaries for communication link and sensor faults. Finally, the simulation results verify the performance of the proposed strategy.

Index Terms—Communication link faults, directed graph, fully distributed control, voltage regulation control.

I. INTRODUCTION

AN microgrid (MG) is a small generation, distribution, and consumption system consisting of a collection of distributed power sources, energy storage systems, energy conversion devices, monitoring and protection devices, and loads [1]. The control structure of an MG is generally divided into three layers: bottom control, secondary control, and tertiary

control. An essential function of the secondary control level is restoring the MGs' voltage [2].

Secondary control can be categorized as centralized, distributed, or decentralized based on the communication method employed. Centralized control enables complex control with high accuracy and speed, making it suitable for small-scale MGs [3]. However, a single point of failure can lead to global control paralysis and reduced reliability. Decentralized control offers fast response time and high reliability but typically lacks accurate global information, resulting in lower control accuracy, susceptibility to interference, stability issues, and limited ability to achieve complex global control objectives [4]. Distributed control, leverages communication between neighboring DGs to achieve consensus through mutual information exchange [5], [6]. It utilizes a distributed local controller approach instead of a central controller, thus avoiding the single point of failure [7]–[9]. The underlying multi-agent system (MAS) consensus algorithm enables each DG to indirectly share global information by communicating only with its neighbors. Reference [10] demonstrates the application of distributed fixed-time and prescribed-time consensus control in the domains of mobile robots and smart grids. Recently, it has become the primary implementation method for secondary control in MGs [11]–[13]. In [14], a distributed consensus protocol is developed to solve the accurate reactive, harmonic and unbalanced power-sharing problems in MG. Consensus-based distributed finite-time regulators are proposed in [15] to coordinate active, frequency and output voltage in islanded MGs. In [16], the problem of distributed secondary control of isolated AC MGs in the presence of external disturbances is studied. However, the secondary control strategies [12]–[16] are based on the premise that the components and communication are perfect.

In practical situations, electrical components such as actuators and sensors may experience failures [17]–[19]. Two distributed control schemes were proposed by [20], [21], respectively, with fault tolerance for various potential faults in sensors and actuators, thus ensuring voltage and frequency regulation of the closed-loop system. Our previous study [22] proposed a fully distributed event-triggered fault-tolerant secondary control method based on information about neighboring distributed generation (DGs). Each DG requires only local information about itself and its neighbors. To achieve AC MG load voltage regulation, [23] proposed an active fault-tolerant event-driven strategy with unknown actuator faults under discrete communication. However, existing fault-tolerant control

strategies applied to MGs generally assume that the communication links are ideal [20]–[23]. The communication between DGs is applied in free space, which is susceptible to physical variations in the communication channel and noise from other sources or channel manipulation from hostile nodes [24], [25]. To achieve high reliability of MG, resilient control of communication failures has become a critical control issue. Distributed control schemes for implementing frequency/voltage restoration and proportional power sharing considering the communication delay problem are proposed in [26]. In [27], a distributed noise-resistant secondary control is proposed for restoring the output voltage and frequency of DG inverter with additive noise. In [28], output voltage and frequency regulation in scenarios where the communication network suffers from both communication delays and switching topologies are investigated. Reference [29] addresses the challenges of current sharing and voltage restoration in islanded DC MGs under heterogeneous communication delays and denial of service (DoS) attacks, providing a novel solution for the first time. This work tackles the complex issues arising from communication delays and cyber-attacks, ensuring efficient and reliable operation of MGs. Inspired by [30], [31], some valuable results were obtained in MG output voltage and frequency restoration control, in the presence of communication failures [24].

However, the resilience regulation of point of common coupling (PCC) voltage in multi-MG systems (MMSs) under communication link and sensor faults remains an unexplored area of research. Existing methods have several limitations that need to be addressed: 1) Previous works [12], [13], [15], [16], [20]–[22], [24], [26]–[28] primarily focused on restoring the output voltage of each DG unit to its nominal value. However, the co-regulation of PCC voltage in MMS is even more critical than regulating the DG output voltage. It is necessary to develop a reasonable system model that reflects the interaction effects between the communication-based PCC voltage control protocol and the DG units in the MMS. 2) Using the conventional consensus tracking method to control the PCC voltages collectively at the reference value would result in no voltage difference between the sub-MGs, thus hindering the power flow between them. Therefore, it is necessary to design reasonable control objectives that address the co-regulation problem of PCC voltages. 3) Furthermore, the PCC voltage regulation problem addressed in this paper is an output feedback tracking problem after feedback linearization. However, the reference-based state observer proposed in previous works [24], [30] is not applicable due to the challenges of full-state unmeasurability and sensor failures. Moreover, the directional communication network and the parameters related to communication and sensor failures are unknown, adding further complexity to the resilient control problem.

Based on the above limitations, we study the AC MG containment-based secondary voltage regulation control with communication link and sensor faults. The main contributions of this paper are summarized as follows:

1) Unlike the traditional consensus-based voltage regulation problem [12], [13], [15], [16], [20]–[22], [24], [26]–[28], we introduce the control objective of containment control in

this paper. The reason is that it is impossible to achieve power flow between sub-MGs if multiple PCC voltages are controlled collectively at the reference value. Therefore, a containment-based distributed controller is proposed to balance the conflicting objectives of voltage regulation and power flow. This controller makes the PCC voltage control within a reasonable range while there is a voltage difference to achieve power flow.

2) Unlike the output voltage regulation problem [12], [13], [15], [16], [20]–[22], [24], [26]–[28], our goal is the regulation problem of the PCC voltage. The feedback linearization technique allows us to deal with nonlinear DG dynamics. Thus, the PCC voltage regulation problem of the AC MG is transformed into a distributed output feedback tracking problem of a linear MAS with nonlinear dynamics. This transformation is an indispensable preprocessing in the design of the control algorithm.

3) The leader-based observer in [27] and [30], [31] is unavailable due to the x_i full-state unmeasurability and sensor fault problems. Therefore, we designed a novel adaptive follower-based observer to handle communication and sensor faults, avoiding the use of global information of directed communication network and fault-related parameters.

The outline of this paper is given below. Section II gives the modeling framework to transform the PCC regulation problem of an AC PCC into a distributed output feedback tracking problem with linear MASs containing unknown nonlinear dynamics. In Section III, some problem statements are made. In Section IV, the main results are established, and a resilient voltage regulation strategy based on containment control is built. Then, Section V verifies the effectiveness of the proposed control method. Section VI concludes this paper.

Notations: Let $I_N \in \mathbb{R}^{N \times N}$ represent the identity matrix, $\lambda_{\max}(*)$ represent the maximum eigenvalue of "*", $\|\cdot\|$ represent the Euclidean norm of vector ".", diag$\{a_1, \ldots, a_N\}$ represent a diagonal matrix, col$\{a_1, a_2, \ldots, a_N\}$ be a column vector, and $\otimes$ represent the Kronecker product.

II. MODELING FRAMEWORK

Considering an MMS containing N sub-MGs, this paper considers the regulation problem of multi-PCC voltages. A sub-MG consists of DGs. The dynamic model of the DG includes droop control, inner-loop voltage and current control, LC filter, containment-based voltage secondary control, and line model, as shown in Fig. 1.
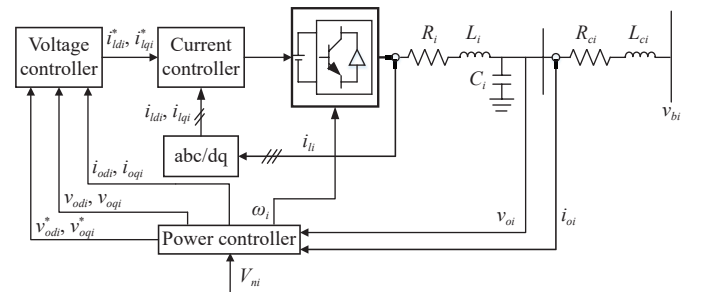
The droop controller dynamics are

Fig. 1.   Block diagram of an inverter-based DG.

$$\omega_i = \omega_{ni} - m_{P_i} P_i$$

$$v_{odi}^* = V_{ni} - n_{Q_i} Q_i$$

$$v_{oqi}^* = 0 \tag{1}$$

where ω_i is the angular frequency of the DG dictated by the primary control, v_{odi}^* is the reference value for the output voltage magnitude that is provided for the internal voltage control loop of the DG, ω_{ni} and V_{ni} are the frequency and the voltage input, m_{P_i} and n_{Q_i} are the droop coefficients, P_i and Q_i are measured active and reactive power at terminals of ith inverter, respectively.

The power controller dynamics are

$$\dot{P}_i = \omega_{c_i} \left(v_{odi} i_{odi} + v_{oqi} i_{oqi} \right) - P_i \omega_{c_i}$$

$$\dot{Q}_i = \omega_{c_i} \left(v_{oqi} i_{odi} - v_{odi} i_{oqi} \right) - Q_i \omega_{c_i} \tag{2}$$

where ω_{ci} is the cutoff frequency of the low-pass filters used in measuring power. v_{odi}, v_{oqi} and i_{odi}, i_{oqi} denote the direct and quadrature components of the output voltage v_{oi} and current i_{oi}, respectively, of the ith inverter.

The voltage and current controller dynamics are

$$\dot{\phi}_{v_{di}} = v_{odi}^* - v_{odi}$$

$$\dot{\phi}_{v_{qi}} = v_{oqi}^* - v_{oqi}$$

$$\dot{\phi}_{i_{di}} = i_{ldi}^* - i_{ldi}$$

$$\dot{\phi}_{i_{qi}} = i_{lqi}^* - i_{lqi}$$

$$i_{ldi}^* = K_{PVi}(v_{odi}^* - v_{odi}) + K_{IVi}\phi_{v_{di}} - \omega_i C_i v_{oqi} + F_{li} i_{odi}$$

$$i_{lqi}^* = K_{PVi}(v_{oqi}^* - v_{oqi}) + K_{IVi}\phi_{v_{qi}} + \omega_i C_i v_{odi} + F_{li} i_{oqi}$$

$$v_{idi}^* = K_{PCi}(i_{ldi}^* - i_{ldi}) + K_{ICi}\phi_{i_{di}} - \omega_i L_i i_{lqi}$$

$$v_{iqi}^* = K_{PCi}(i_{lqi}^* - i_{lqi}) + K_{ICi}\phi_{i_{qi}} + \omega_i L_i i_{ldi} \tag{3}$$

where $\phi_{v_{di}}$, $\phi_{v_{qi}}$ are auxiliary state variables in the voltage controller. $\phi_{i_{di}}$, $\phi_{i_{qi}}$ are auxiliary state variables in the current controller. i_{ldi}^*, i_{lqi}^* are current reference in the current controller. i_{ldi} and i_{lqi} are filter current components. K_{PVi} and K_{IVi} are proportion and integral parameters in the voltage controller, respectively. $\phi_{v_{di}}$, $\phi_{v_{qi}}$ are auxiliary state variables in the voltage controller. F_{li} is feedforward parameter in the voltage controller. C_i and L_i are filter capacitor and inductance, respectively. K_{PCi} and K_{ICi} are proportion and integral parameters in the current controller, respectively. $\phi_{i_{di}}$, $\phi_{i_{qi}}$ are auxiliary state variables in the current controller.

The output LC filter and connector dynamics are

$$\dot{i}_{ldi} = -\frac{R_i}{L_i} i_{ldi} + \omega_i i_{lqi} + \frac{1}{L_i} v_{idi} - \frac{1}{L_i} v_{odi}$$

$$\dot{i}_{lqi} = -\frac{R_i}{L_i} i_{lqi} - \omega_i i_{ldi} - \frac{1}{L_i} v_{oqi}$$

$$\dot{v}_{odi} = \omega_i v_{oqi} + \frac{1}{C_i} i_{ldi} - \frac{1}{C_i} i_{odi}$$

$$\dot{v}_{oqi} = -\omega_i v_{odi} + \frac{1}{C_i} i_{lqi} - \frac{1}{C_i} i_{oqi}$$

$$\dot{i}_{odi} = \frac{1}{L_{c_i}} v_{odi} - \frac{R_{c_i}}{L_{c_i}} i_{odi} - \frac{1}{L_{c_i}} v_{bdi} + \omega_i i_{oqi}$$

$$\dot{i}_{oqi} = \frac{1}{L_{c_i}} v_{oqi} - \frac{R_{c_i}}{L_{c_i}} i_{oqi} - \frac{1}{L_{c_i}} v_{bqi} - \omega_i i_{odi} \tag{4}$$

where R_i is filter resistance. v_{idi}, v_{iqi} are output components of the current controller. v_{bdi}, v_{bqi} are the components of the PCC voltage. L_{c_i}, R_{c_i} are inductance, resistance of the line between the PCC and the inverter output, respectively.

The nonlinear dynamic model of the AC MG in a compact form is

$$\dot{z}_i = f_i(z_i) + k_i(z_i)J_i + g_i(z_i)u_i$$

$$y_i = d_i(z_i) + v_{li} \tag{5}$$

where the state vector is

$$z_i = [\delta_i, P_i, Q_i, \phi_{v_{di}}, \phi_{v_{qi}}, \phi_{i_{di}}, \phi_{i_{qi}}, i_{ldi}, i_{lqi}, v_{odi}, v_{oqi}, i_{odi}, i_{oqi}]^T \tag{6}$$

and $J_i = [\omega_{com}, v_{bdi}, v_{bqi}]$. Detailed expressions for $f_i(z_i)$, $g_i(z_i)$, and $k_i(z_i)$ can be extracted from (1)−(4). Moreover, $d_i(z_i)$ is set to v_{odi}. y_i is set to v_{bdi}. v_{li} represents the voltage of the line between the PCC and the inverter output.

Then, by feedback linearization, we have

$$\ddot{y}_i = L_{F_i}^2 d_i + L_{g_i} L_{F_i} d_i V_{ni} + \ddot{v}_{li} = u_i + \ddot{v}_{li} \tag{7}$$

where $F_i = f_i(z_i) + k_i(z_i)J_i$, $L_{F_i} d_i = \frac{\partial d_i}{\partial x_i} F_i$ and $L_{F_i}^2 d_i = L_{F_i}(L_{F_i} d_i) = \frac{\partial L_{F_i} d_i}{\partial x_i} F_i$ are the Lie derivatives of d_i along F_i.

The control input V_{ni} is implemented by u_i as

$$V_{ni} = (L_{g_i} L_{F_i} d_i)^{-1}(-L_{F_i}^2 d_i + u_i). \tag{8}$$

It is difficult to obtain the value of $\dot{v}_{bdi}$ in practice, the design of the control algorithm using only v_{bdi} instead of x_i, where x_i is translated from (7) as follows:

$$\begin{cases} \dot{x}_i(t) = Ax_i(t) + B(u_i + \ddot{v}_{li}), & i = 1,\dots,N \\ y_i(t) = Cx_i(t) \end{cases} \tag{9}$$

where $x_i = [v_{bdi}, \dot{v}_{bdi}]^T$, $A = \begin{bmatrix} 0 & 1 \\ 0 & 0 \end{bmatrix}$, $B = [0,1]^T$, $C = [1,0]$.

Remark 1: Unlike the traditional output voltage v_{odi} regulation problem in [12], [13], [15], [16], [20]–[22], [24], [26]–[28], we address the PCC voltage v_{bdi} regulation problem for AC MGs. Moreover, due to the x_i full-state unmeasurability, the state-based controller cannot achieve v_{bdi} regulation. In the input-output feedback linearization (7), repeated differentiation concerning time generates the direct relationship between the dynamics of v_{bdi} (or equivalently y_i) and the control input V_{ni}. The v_{bdi} regulation problem is transformed into a distributed output feedback tracking problem with linear MAS, where the system contains nonlinear dynamics $\ddot{v}_{li}$. Moreover, an appropriate auxiliary controller u_i is designed so that v_{bdi} regulation is achieved using V_{ni}. The design of controller u_i depends on state observer $\hat{x}_i$, while the design of $\hat{x}_i$ depends on v_{bdi}.

The containment-based voltage controller for each sub-MGs bound voltages within a reasonable range. The virtual leaders serve as the upper and lower boundaries of the specified voltage, as follows:

$$\dot{x}_m(t) = Ax_m(t), \qquad m = N+1, \ N+2 \qquad (10)$$

where $x_m = [v_{ref_{m-N}}, 0]^T$. Define $x_{ref} = \text{col}\{x_{N+1}, x_{N+2}\}$, and v_{ref_1}, v_{ref_2} represent the upper and lower boundaries of the voltage regulation, respectively.

III. PROBLEM STATEMENT

The N sub-MGs upper communication graph can be modeled by $\mathcal{G}(\mathcal{C}, \mathcal{T})$. $\mathcal{C} = \{c_1, c_2, \ldots, c_N\}$ is the node set, $\mathcal{T} \subseteq \mathcal{C} \times \mathcal{C}$ is the edge set. The weighted adjacency matrix $\mathcal{D} = [a_{ij}] \in \mathbb{R}^{(N+2) \times (N+2)}$ is defined by $a_{ij} = 1$, if $(c_i, c_j) \in \mathcal{T}$, otherwise, $a_{ij} = 0$. The nonsymmetric Laplacian matrix $\mathcal{L} = [\mathcal{L}_{ij}]$ of $\mathcal{G}$ is defined as $\mathcal{L}_{ii} = \sum_{j=1}^{N+2} a_{ij}$ and $\mathcal{L}_{ij} = -a_{ij}$, where $i \neq j$.

Assumption 1: The communication topology between the PCC terminals of the sub-MG is directed. At least one virtual leader's dynamics is directed to all sub-MG's PCC terminals.

Assumption 1 is the basic standard assumption of MASs containment control.

In this paper, the faults are modeled as follows:
1) The communication links faults:

$$\bar{a}_{ij}(t) = a_{ij} + \delta_{ij}^a(t), \quad i = 1, 2, \ldots, N, \ j = 1, 2, \ldots, N+2 \qquad (11)$$

where $\delta_{ij}^a(t)$ denotes the corrupted weight caused by communications faults. From the fault model (11), the communication link weights become time-varying and unknown due to $\delta_{ij}^a(t)$.

2) The sensors faults:

$$y_i(t) = Cx_i(t) + h_i(t), \qquad i = 1, 2, \ldots, N \qquad (12)$$

where h_i is the unknown sensor fault.

Assumption 2: The communication link faults $\delta_{ij}^a(t)$, $i = 1, 2, \ldots, N$, $j = 1, 2, \ldots, N+2$, and their derivatives are bounded but unknown. The signs of $\bar{a}_{ij}$ are the same to those of a_{ij}, respectively.

Assumption 3: The time derivative of sensor fault is bounded, i.e., $\|\dot{h}_i(t)\| \leq \bar{h}_i$.

Remark 2: An MG includes multiple power sources, actuators, sensors, and communication networks. Actuator faults can adversely affect the stability and performance of the MG. These faults can result in erroneous decision making and operation, impacting the effectiveness of the MG's energy management and overall operation. Sensor faults can lead to inaccurate sensing and collection of environmental and energy data within the MG. This, in turn, affects the system's dispatch and control strategy. Furthermore, communication among DGs in the MG occurs wirelessly and is susceptible to physical changes in the communication channel, noise interference from other sources, or malicious manipulation by hostile nodes. In this paper, we focus on sensor and communication fault issues. Assumption 2 guarantees the boundedness of the considered communication link faults and their derivatives, found in [30]. Assumption 3 ensures the boundedness of the sensor derivatives, found in [18].

Due to the communication link faults (11), the Laplace matrix is redefined as $\mathcal{L}(t) = \mathcal{J}(t) - \mathcal{D}(t)$, where $\mathcal{D}(t) = [\bar{a}_{ij}(t)]$ is the adjacency matrix and $\mathcal{J}(t) = \text{diag}\{\sum_{j \in N_i} \bar{a}_{ij}(t)\}$ is the indegree matrix.

Then, $\mathcal{L}(t)$ is defined as

$$\mathcal{L}(t) = \begin{bmatrix} 0_{2 \times 2} & 0_{2 \times N} \\ \mathcal{L}_2(t) & \mathcal{L}_1(t) \end{bmatrix} \qquad (13)$$

where $\mathcal{L}_2(t) \in \mathbb{R}^{N \times 2}$, $\mathcal{L}_1(t) \in \mathbb{R}^{N \times N}$. The real part of each eigenvalue of $\mathcal{L}_1(t)$ is positive. It is easy to verify that $\mathcal{L}_1(t)$ is a nonsingular M-matrix.

Lemma 1 [30]: Assume that Assumptions 1 and 2 hold. On this basis, there exists a positive infinite diagonal matrix $\mathcal{K}(t)$ such that $\mathcal{K}(t)\mathcal{L}_1(t) + \mathcal{L}_1^T(t)\mathcal{K}(t) = \mathcal{N}(t)$ holds, where $\mathcal{N}(t)$ is positive. Then, $\mathcal{K}(t)$ and $\dot{\mathcal{K}}(t)$ are bounded.

Lemma 2 [32]: The matched uncertainty $f_i(x_i)$ can be linearly parameterized by a neural network as

$$f_i(x_i) = W_i^T \varphi_i(x_i) + \varepsilon_i \qquad (14)$$

where $W_i \in \mathbb{R}^{s \times 1}$ is an unknown constant ideal weight matrix that satisfies $\|W_i\| \leq \check{W}_i$ with $\check{W}_i$ being a positive constant, $\varphi_i(\cdot) : \mathbb{R}^n \to \mathbb{R}^s$ is a known vector function of the form $\varphi_i(x_i) = [\varphi_{i1}(x_i), \varphi_{i2}(x_i), \ldots, \varphi_{is}(x_i)]^T$ and satisfies $\|\varphi_i\| \leq \check{\varphi}_i$ with being $\check{\varphi}_i$ a positive constant, ε_i is the approximation error satisfying $\|\varepsilon_i\| \leq \check{\varepsilon}_i$ with being $\check{\varepsilon}_i$ a positive constant.

Then, by Lemma 1, we obtain

$$\ddot{v}_{li} = W_i^T \varphi_i(x_i) + \varepsilon_i. \qquad (15)$$

The dynamic model of the ith agent is

$$\begin{cases} \dot{x}_i(t) = Ax_i(t) + B(u_i + W_i^T \varphi_i(x_i) + \varepsilon_i) \\ y_i^F(t) = Cx_i(t) + h_i(t). \end{cases} \qquad (16)$$

Remark 3: The reference-based state observer in [30] is unavailable due to the x_i full-state unmeasurability and sensor fault issues. Moreover, the boundaries of the fault-related parameters of the directed communication network and the communication and sensors are unknown. Therefore, we next design a new adaptive follower-based observer to handle communication and sensor faults.

IV. MAIN RESULT

The purpose of this section is to co-regulate the PCC voltage v_{bdi}, $i = 1, 2, \ldots, N$ in an MMS to a given region. Besides, from the practical needs of the power system, the proposed secondary control protocol does not depend on the global information of the directed communication network and the boundary of the fault factor. We design a containment-based secondary voltage strategy for communication link and sensor faults for a MMS, as shown in Fig. 2. For simplicity, only one DG is shown in each sub-MG.

The state observer $\hat{x}_i$ to estimates x_i, $i = 1, 2, \ldots, N$ is as follows:

$$\begin{cases} \dot{\hat{x}}_i(t) = A\hat{x}_i(t) + \hat{u}_i + B\hat{W}_i^T \varphi_i(\hat{x}_i) - L(\hat{y}_i - y_i) \\ \hat{y}_i(t) = C\hat{x}_i(t) + \hat{h}_i \end{cases} \qquad (17)$$

where

$$\dot{\hat{h}}_i = G(\hat{y}_i(t) - y_i(t)) \qquad (18)$$

and $\hat{x}_i(t)$, $\hat{h}_i$, $\hat{y}_i(t)$, $\hat{W}_i$ and $\varphi_i(\hat{x}_i)$ are the estimations of $x_i(t)$, h_i, $y_i(t)$, W_i and $\varphi_i(x_i)$, respectively. $L \in \mathbb{R}^{2 \times 1}$ is the observer gain. G is estimator gains.

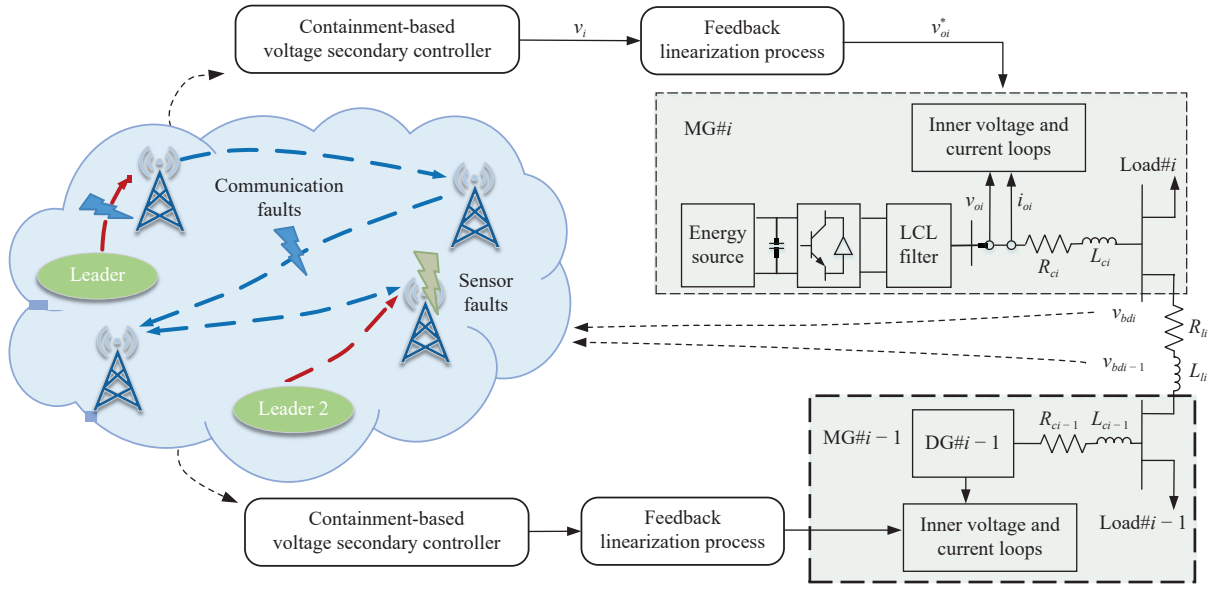Let the observer controller $\hat{u}_i$ in (17) be

Fig. 2.   Block diagram of an MMS and the proposed containment-based secondary voltage regulation strategy for communication link and sensor faults.

$$\hat{u}_i = -c(\phi_i + \upsilon_i)P\vartheta_i(t) \tag{19}$$

where

$$\dot{\phi}_i = -\nu_{\phi_i}(\phi_i - 1) + \vartheta_i^T(t)PP\vartheta_i(t) \tag{20}$$

$$\upsilon_i = \vartheta_i^T(t)P\vartheta_i(t) \tag{21}$$

where c, ν_{ϕ_i} are positive constants. Moreover, $\vartheta_i = \sum_{j=1}^{N+2} \bar{a}_{ij} \times (\hat{x}_i(t) - \hat{x}_j(t))$. Moreover, $\phi_i(0) \geq 1$. Then, it is easy to obtain $\phi_i(t) \geq 1$ for any $t > 0$.

Under Assumption 1, $-\mathcal{L}_1^{-1}(t)\mathcal{L}_2(t)x_{ref}$ is within the convex hull spanned by the multiple leaders. Let

$$\bar{x} = -\mathcal{L}_1^{-1}(t)\mathcal{L}_2(t)x_{ref}. \tag{22}$$

Define $\epsilon = \text{col}\{\epsilon_1(t), \epsilon_2(t), \ldots, \epsilon_N(t)\}$, then

$$\epsilon = \hat{x} + \bar{x} = \hat{x} + (\mathcal{L}_1^{-1}(t)\mathcal{L}_2(t) \otimes I_n)x_{ref} \tag{23}$$

where $\hat{x} = \text{col}\{\hat{x}_1(t), \hat{x}_2(t), \ldots, \hat{x}_N(t)\}$. The global disagreement vector ϑ of the graph $\mathbb{G}$ can be written as

$$\vartheta = (\mathcal{L}_1(t) \otimes I_2)\hat{x} + (\mathcal{L}_2(t) \otimes I_2)x_{ref} \tag{24}$$

where $\vartheta = \text{col}\{\vartheta_1(t), \vartheta_2(t), \ldots, \vartheta_N(t)\}$.

Remark 4: It can be seen from Fig. 2 that power cannot flow between DGs if the PCC voltages v_{bdi}, $i = 1, 2, \ldots, N$ are controlled at their nominal value. Therefore, this paper introduces the control objective of containment control. On this basis, a secondary voltage regulation strategy based on containment control is proposed. The strategy limits each PCC voltage v_{bdi} to a reasonable range while having a voltage difference between sub-MGs to allow power flow.

Then,

$$\dot{\hat{x}}_i(t) = A\hat{x}_i(t) - c(\phi_i + \upsilon_i)P\vartheta_i(t) + B\hat{W}_i^T\varphi_i(\hat{x}_i)$$
$$- LC\alpha_i - L\tilde{h}_i \tag{25}$$

where $\alpha_i = \hat{x}_i - x_i$, $\tilde{h}_i = \hat{h}_i - h_i$, and

$$\dot{\hat{W}}_i = \Gamma_{\hat{W}_i}[-(\chi_4 + \chi_5)\varphi_i(\hat{x}_i)\varphi_i^T(\hat{x}_i)\hat{W}_i - 2\iota_{\hat{W}_i}\varphi_i(\hat{x}_i)R^T\tilde{y}_i^T$$
$$- k_{\hat{W}_i}\hat{W}_i] \tag{26}$$

where $\Gamma_{\hat{W}_i}$, $\iota_{\hat{W}_i} > 0$. The parameters $R \in \mathbb{R}^{2 \times 1}$, $k_{\hat{W}_i} > 0$ will be determined later.

Due to $\vartheta = (\mathcal{L}_1(t) \otimes I_2)\epsilon$, we obtain the dynamics of ϑ as follows:

$$\dot{\vartheta} = (\dot{\mathcal{L}}_1(t) \otimes I_2)\epsilon + (I_N \otimes A)\vartheta - [c\mathcal{L}_1(t)(\phi + \upsilon) \otimes P]\vartheta$$
$$+ (\mathcal{L}_1(t) \otimes B)\hat{W}^T\varphi(\hat{x})(\mathcal{L}_1(t) \otimes LC)\alpha$$
$$- (\mathcal{L}_1(t) \otimes L)\tilde{h} \tag{27}$$

where $\phi = \text{diag}\{\phi_1, \phi_2, \ldots, \phi_N\}$, $\upsilon = \text{diag}\{\upsilon_1, \upsilon_2, \ldots, \upsilon_N\}$, $\hat{W} = \text{diag}\{\hat{W}_1, \hat{W}_2, \ldots, \hat{W}_N\}$, $\varphi(\hat{x}) = \text{col}\{\varphi_1(\hat{x}_1), \varphi_2(\hat{x}_2), \ldots, \varphi_N(\hat{x}_N)\}$, $\alpha = \text{col}\{\alpha_1, \alpha_2, \ldots, \alpha_N\}$, $\tilde{h} = \text{col}\{\tilde{h}_1, \tilde{h}_2, \ldots, \tilde{h}_N\}$.

Let the auxiliary control u_i in (9) be

$$u_i = -c(\phi_i + \upsilon_i)B^T P\vartheta_i(t). \tag{28}$$

It is easy to obtain

$$\begin{cases} \dot{\alpha}_i = (A - LC)\alpha_i + B(\hat{W}_i^T\varphi_i(\hat{x}_i) - W_i^T\varphi_i(x) - \varepsilon_i) \\ \quad - L\tilde{h}_i + c(I_2 - BB^T)(\phi_i + \upsilon_i)P\vartheta_i(t) \\ \dot{\tilde{h}}_i = GC\alpha_i(t) + G\tilde{h}_i - \dot{h}_i. \end{cases} \tag{29}$$

Define $\tilde{h} = \text{col}\{\tilde{h}_1, \tilde{h}_2, \ldots, \tilde{h}_N\}$. It shows that

$$\begin{cases} \dot{\alpha} = (I_N \otimes (A - LC))\alpha \\ \quad + (I_N \otimes B)(\hat{W}^T\varphi(\hat{x}) - W^T\varphi(x) - \varepsilon) \\ \quad + (I_N \otimes L)\tilde{h} + [c(\phi + \upsilon) \otimes (I_2 - BB^T)P]\vartheta \\ \dot{\tilde{h}} = (I_N \otimes GC)\alpha + (I_N \otimes G)\tilde{h} - \dot{h} \end{cases} \tag{30}$$

where $\varphi(x) = \text{col}\{\varphi_1(x_1), \varphi_2(x_2), \ldots, \varphi_N(x_N)\}$, $W = \text{diag}\{W_1, W_2, \ldots, W_N\}$, $h = \text{col}\{h_1, h_2, \ldots, h_N\}$, $\varepsilon = \text{col}\{\varepsilon_1, \varepsilon_2, \ldots, \varepsilon_N\}$.

Let $\eta = \text{col}\{\alpha, \tilde{h}\}$, then

$$\dot{\eta} = \mathcal{A}\eta + \mathcal{B}(\hat{W}^T\varphi(\hat{x}) - W^T\varphi(x)) - \beta + \mathcal{T} \tag{31}$$

where

$$\mathcal{A} = \begin{bmatrix} I_N \otimes (A - LC) & I_N \otimes L \\ I_N \otimes GC & I_N \otimes G \end{bmatrix} \tag{32}$$

$\mathcal{B} = [I_N \otimes B, 0]^T$, $\beta = [(I_N \otimes B)\varepsilon, \dot{h}]^T$, $\mathcal{T} = [[c(\phi + \upsilon) \otimes (I_2 - BB^T)P]\vartheta, 0]^T$.

Theorem 1: Suppose Assumptions 1−3 hold, and there exist appropriate χ_m, $m = 1, 2, 3, 4, 5, 11, 12$. $P > 0$, $\Gamma > 0$, $\mathcal{M} > 0$, R, G and L are with appropriate dimensions such that

$$PA^T + AP - PP + \eta I_2 = 0 \tag{33}$$

$$\Gamma \mathcal{A} + \mathcal{A}^T \Gamma + (\chi_1^{-1} + \chi_2^{-1} c)\eta^T \Gamma \Gamma \eta$$
$$+ \chi_3^{-1} \eta^T \Gamma \mathcal{B} \mathcal{B}^T \Gamma \eta + \mathcal{H} = -\mathcal{V} \tag{34}$$

where

$$\Gamma = \begin{bmatrix} I_n \otimes \Gamma_{11} & I_n \otimes \Gamma_{12} \\ I_n \otimes \Gamma_{12} & I_n \otimes \Gamma_{22} \end{bmatrix} \tag{35}$$

$\mathcal{H} = \mathrm{diag}\{\chi_4^{-1}\mathcal{M}\mathcal{M}^T + \chi_{11}^{-1}C^T L^T LC, \chi_5^{-1}\mathcal{U}\mathcal{U}^T + \chi_{12}^{-1}L^T L\}$, $\mathcal{M} = \Gamma_{11} - \iota_{\hat{W}_i}C^T$, $\mathcal{U} = \Gamma_{12}^T - \iota_{\hat{W}_i}R^T$. Then, the containment error vector will converge exponentially to a bounded domain.

Proof: Consider the following Lyapunov function candidate:

$$V = V_1 + V_2 \tag{36}$$

where

$$V_1 = \eta^T \Gamma \eta + \frac{1}{2} tr(\tilde{W}^T \Gamma_{\hat{W}}^{-1} \tilde{W}) \tag{37}$$

$$V_2 = \frac{1}{2} \sum_{i=1}^{N} k_i(2\phi_i + \upsilon_i)\upsilon_i + \frac{1}{2} \sum_{i=1}^{N} s_i(\phi_i - \bar{\phi}_i)^2 \tag{38}$$

where $\tilde{W} = \mathrm{diag}\{\tilde{W}_1, \tilde{W}_2, \ldots, \tilde{W}_N\}$, $\tilde{W}_i = \hat{W}_i - W_i$, $\Gamma_{\hat{W}} = \mathrm{diag}\{\Gamma_{\hat{W}_1}, \Gamma_{\hat{W}_2}, \ldots, \Gamma_{\hat{W}_N}\}$. s_i, $\bar{\phi}_i$ are positive constants to be determined later. Then, it is not difficult to obtain V is the positive definite.

Taking the derivative of V_1, from (26) and (31), we obtain that

$$\dot{V}_1 = 2\eta^T \Gamma \dot{\eta} + tr(\tilde{W}^T \Gamma_{\hat{W}}^{-1} \dot{\tilde{W}}). \tag{39}$$

Define $\tilde{\varphi} = \mathrm{col}\{\tilde{\varphi}_1, \tilde{\varphi}_2, \ldots, \tilde{\varphi}_N\}$, $\tilde{\varphi}_i = \varphi_i(\hat{x}_i) - \varphi_i(x_i)$,

$$2\eta^T \Gamma \dot{\eta} = 2\eta^T \Gamma \mathcal{A} \eta - 2\eta^T \Gamma \beta + 2\eta^T \Gamma \mathcal{T}$$
$$+ 2\eta^T \Gamma \mathcal{B}(\hat{W}^T \varphi(\hat{x}) - W^T \varphi(x))$$
$$= 2\eta^T \Gamma \mathcal{A} \eta - 2\eta^T \Gamma \beta + 2\eta^T \Gamma \mathcal{T} + 2\eta^T \Gamma \mathcal{B} W^T \tilde{\varphi}$$
$$+ 2 \sum_{i=1}^{N} (\alpha_i^T \Gamma_{11} + \tilde{h}_i^T \Gamma_{12}^T) B \tilde{W}_i^T \varphi_i(\hat{x}_i)$$
$$= 2\eta^T \Gamma \mathcal{A} \eta - 2\eta^T \Gamma \beta + 2\eta^T \Gamma \mathcal{T} + 2\eta^T \Gamma \mathcal{B} W^T \tilde{\varphi}$$
$$+ 2 \sum_{i=1}^{N} \iota_{\hat{W}_i} R^T (\hat{y}_i - y_i)^T \tilde{W}_i^T \varphi_i(\hat{x}_i)$$
$$+ 2 \sum_{i=1}^{N} \alpha_i^T \mathcal{M} \tilde{W}_i^T \varphi_i(\hat{x}_i) + 2 \sum_{i=1}^{N} \tilde{h}_i^T \mathcal{U} \tilde{W}_i^T \varphi_i(\hat{x}_i) \tag{40}$$

$\mathcal{M} = \Gamma_{11} - \iota_{\hat{W}_i}C^T$, $\mathcal{U} = \Gamma_{12}^T - \iota_{\hat{W}_i}R^T$, Using the Young's inequality, for any positive constants χ_m, $m = 1, 2, \ldots, 5$, one has

$$-2\eta^T \Gamma \beta \le \chi_1^{-1} \eta^T \Gamma \Gamma \eta + \chi_1 \beta^T \beta \tag{41}$$

$$2\eta^T \Gamma \mathcal{T} \le \chi_2^{-1} c\eta^T \Gamma \Gamma \eta + \chi_2 \|I_2$$
$$- BB^T\|^2 c \sum_{i=1}^{N} (\phi_i + \upsilon_i)^2 \vartheta_i^T PP \vartheta_i \tag{42}$$

$$2\eta^T \Gamma \mathcal{B} W^T \tilde{\varphi} \le \chi_3^{-1} \eta^T \Gamma \mathcal{B} \mathcal{B}^T \Gamma \eta + \chi_3 \tilde{\varphi}^T W W^T \tilde{\varphi} \tag{43}$$

$$2\alpha_i^T \mathcal{M} \tilde{W}_i^T \varphi_i(\hat{x}_i) \le \chi_4^{-1} \alpha_i^T \mathcal{M} \mathcal{M}^T \alpha_i$$
$$+ \chi_4 \varphi_i^T(\hat{x}_i) \tilde{W}_i \tilde{W}_i^T \varphi_i(\hat{x}_i) \tag{44}$$

and

$$2\tilde{h}_i^T \mathcal{U} \tilde{W}_i^T \varphi_i(\hat{x}_i) \le \chi_5^{-1} \tilde{h}_i^T \mathcal{U} \mathcal{U}^T \tilde{h}_i$$
$$+ \chi_5 \varphi_i^T(\hat{x}_i) \tilde{W}_i \tilde{W}_i^T \varphi_i(\hat{x}_i). \tag{45}$$

Applying (41)−(45) to (40), for any positive constants χ_6 and χ_7, one can obtain that

$$tr(\tilde{W}^T \Gamma_{\hat{W}}^{-1} \dot{\tilde{W}}) = -\sum_{i=1}^{N} (\chi_4 + \chi_5)\varphi^T(\hat{x}_i)\hat{W}_i \tilde{W}_i^T \varphi(\hat{x}_i)$$
$$- 2 \sum_{i=1}^{N} tr(\iota_{\hat{W}_i} \tilde{W}_i^T \varphi_i(\hat{x}_i)R^T(\hat{y}_i - y_i)^T)$$
$$- \sum_{i=1}^{N} k_{\hat{W}_i} tr(\tilde{W}_i^T \hat{W}_i)$$
$$\le -\sum_{i=1}^{N} (\chi_4 + \chi_5)\varphi^T(\hat{x}_i)\tilde{W}_i \tilde{W}_i^T \varphi(\hat{x}_i)$$
$$+ \sum_{i=1}^{N} \left[\frac{(\chi_4 + \chi_5)\chi_6}{2}\varphi_{mi}^4 + \frac{\chi_7}{2}k_{\hat{W}_i} \right] \breve{W}_i^2$$
$$- \sum_{i=1}^{N} \left[(1 - \frac{1}{2\chi_7})k_{\hat{W}_i} - \frac{(\chi_4 + \chi_5)}{2\chi_6} \right] \|\tilde{W}_i\|_F^2$$
$$- 2 \sum_{i=1}^{N} tr(\iota_{\hat{W}_i} \tilde{W}_i^T \hat{\varphi}_i R^T(\hat{y}_i - y_i)^T). \tag{46}$$

Then,

$$tr(\tilde{W}^T \Gamma_{\hat{W}}^{-1} \dot{\tilde{W}}) + 2\eta^T \Gamma \dot{\eta}$$
$$\le 2\eta^T \Gamma \mathcal{A} \eta + (\chi_1^{-1} + \chi_2^{-1} c)\eta^T \Gamma \Gamma \eta + \chi_1 \beta^T \beta$$
$$+ \chi_3^{-1} \eta^T \Gamma \mathcal{B} \mathcal{B}^T \Gamma \eta$$
$$+ \chi_2 c \|I_2 - BB^T\|^2 \sum_{i=1}^{N} (\phi_i + \upsilon_i)^2 \vartheta_i^T PP \vartheta_i$$
$$+ \chi_4^{-1} \sum_{i=1}^{N} \alpha_i^T \mathcal{M} \mathcal{M}^T \alpha_i + \chi_5^{-1} \sum_{i=1}^{N} \tilde{h}_i^T \mathcal{U} \mathcal{U}^T \tilde{h}_i \tag{47}$$
$$+ \sum_{i=1}^{N} \left[\frac{(\chi_4 + \chi_5)\chi_6}{2}\varphi_{mi}^4 + 4\chi_3 \varphi_{mi}^2 + \frac{\chi_7}{2}k_{\hat{W}_i} \right] \breve{W}_i^2$$
$$- \sum_{i=1}^{N} \left[(1 - \frac{1}{2\chi_7})k_{\hat{W}_i} - \frac{(\chi_4 + \chi_5)}{2\chi_6} \right] \|\tilde{W}_i\|_F^2. \tag{48}$$

Next, taking the derivative of V_2, from (20) and (21), we obtain that

$$\dot{V}_2 = \sum_{i=1}^{N} k_i(\phi_i + v_i)\dot{v}_i + \sum_{i=1}^{N} k_i\dot{\phi}_i v_i$$
$$+ \sum_{i=1}^{N} s_i(\phi_i - \bar{\phi}_i)\dot{\phi}_i + \frac{1}{2}\sum_{i=1}^{N} \dot{k}_i(2\phi_i + v_i)v_i. \quad (49)$$

Then,

$$\dot{V}_2 = \sum_{i=1}^{N} k_i(\phi_i + v_i)\dot{v}_i$$
$$= \vartheta^T[(\phi + v)\mathcal{K}(t)\dot{\mathcal{L}}_1(t) \otimes P]\epsilon$$
$$+ \vartheta^T[(\phi + v)\mathcal{K}(t) \otimes (PA + A^T P)]\vartheta$$
$$- 2c\vartheta^T[(\phi + v)\mathcal{K}(t)\mathcal{L}_1(t)(\phi + v) \otimes PBB^T P]\vartheta$$
$$+ 2\vartheta^T[(\phi + v)\mathcal{K}(t)\mathcal{L}_1(t) \otimes PB]\hat{W}^T\varphi(\hat{x})$$
$$- 2\vartheta^T[(\phi + v)\mathcal{K}(t)\mathcal{L}_1(t) \otimes PLC]\alpha$$
$$- 2\vartheta^T[(\phi + v)\mathcal{K}(t)\mathcal{L}_1(t) \otimes PL]\tilde{h}. \quad (50)$$

From (23) and (24), we obtain $\|\epsilon\| \leq \|\mathcal{L}_1^{-1}(t)\|\|\vartheta\|$. Define $\mathcal{K}_m$ as the lower bound of $\mathcal{K}(t)$. For any positive constant χ_8, we obtain

$$2\vartheta^T[(\phi + v)\dot{\mathcal{L}}_1(t) \otimes P]\epsilon$$
$$\leq \frac{\chi_8}{\mathcal{K}_m\lambda_{\min}(P)}\vartheta^T[(\phi + v)\mathcal{K}(t) \otimes PP]\vartheta$$
$$+ \frac{\lambda_{\max}(\dot{\mathcal{L}}_1^T(t)\dot{\mathcal{L}}_1(t))\|\mathcal{L}_1^{-1}(t)\|^2}{\chi_8\mathcal{K}_m\lambda_{\min}(P)}$$
$$\times \vartheta^T[(\phi + v)\mathcal{K}(t) \otimes PP]\vartheta. \quad (51)$$

By Lemma 2, the minimum eigenvalue of $\mathcal{N}(t)$ is denoted by λ_0, it follows:

$$-2c\vartheta^T[(\phi + v)\mathcal{K}(t)\mathcal{L}_1(t)(\phi + v) \otimes PP]\vartheta$$
$$= -c\vartheta^T[(\phi + v)(\mathcal{K}(t)\mathcal{L}_1(t) + \mathcal{L}_1^T(t)\mathcal{K}(t))(\phi + v)$$
$$\otimes PP]\vartheta$$
$$\leq -c\lambda_0\sum_{i=1}^{N}(\phi_i + v_i)^2\vartheta_i^T PP\vartheta_i. \quad (52)$$

Defining the maximum eigenvalue of $\mathcal{K}(t)\mathcal{L}_1(t)\mathcal{L}_1^T(t)\mathcal{K}(t)$ as λ_Ξ, for any positive constants χ_9 and χ_{10}, one obtains

$$2\vartheta^T[(\phi + v)\mathcal{K}(t)\mathcal{L}_1(t) \otimes PB]\hat{W}^T\varphi(\hat{x})$$
$$= 2\vartheta^T[(\phi + v)\mathcal{K}(t)\mathcal{L}_1(t) \otimes PB][\tilde{W}^T\varphi(\hat{x}) + W^T\varphi(\hat{x})]$$
$$\leq \|B^T\|^2\sum_{i=1}^{N}(\chi_9\varphi_{mi}^2 + \chi_{10})\lambda_\Xi(\phi_i + v_i)^2\vartheta_i^T PP\vartheta_i$$
$$+ \chi_9^{-1}\sum_{i=1}^{N}\|\tilde{W}_i\|_F^2 + \chi_{10}^{-1}\sum_{i=1}^{N}\varphi_{mi}^2\check{W}_i^2. \quad (53)$$

Moreover, for any positive constants χ_{11} and χ_{12}, it is easy to get

$$-2\vartheta^T[(\phi + v)\mathcal{K}(t)\mathcal{L}_1(t) \otimes PLC]\alpha$$
$$\leq \chi_{11}\sum_{i=1}^{N}\lambda_\Xi(\phi_i + v_i)^2\vartheta_i^T PP\vartheta_i$$
$$+ \chi_{11}^{-1}\sum_{i=1}^{N}\alpha_i^T C^T L^T LC\alpha_i \quad (54)$$

and

$$-2\vartheta^T[(\phi + v)\mathcal{K}(t)\mathcal{L}_1(t) \otimes PL]\tilde{h}$$
$$\leq \chi_{12}\sum_{i=1}^{N}\lambda_\Xi(\phi_i + v_i)^2\vartheta_i^T PP\vartheta_i + \chi_{12}^{-1}\sum_{i=1}^{N}\tilde{h}_i^T L^T L\tilde{h}_i. \quad (55)$$

Since $s_i > 0$ is sufficiently large such that $s_i \geq \max_{i=1,2,...,N}\{k_i\}$ holds, we obtain

$$\sum_{i=1}^{N} k_i\dot{\phi}_i v_i + \sum_{i=1}^{N} s_i(\phi_i - \bar{\phi}_i)\dot{\phi}_i$$
$$= \vartheta^T[v\mathcal{K}(t) \otimes PP]\vartheta - \sum_{i=1}^{N} k_i v_{\phi i}v_i(\phi_i - 1)$$
$$+ \vartheta^T[s(\phi - \bar{\phi}) \otimes PP]\vartheta - \sum_{i=1}^{N} s_i v_{\phi i}(\phi_i - \bar{\phi}_i)(\phi_i - 1)$$
$$\leq \vartheta^T[s(v + \phi - \bar{\phi})\mathcal{K}(t) \otimes PP]\vartheta$$
$$- \sum_{i=1}^{N} k_i v_{\phi i}(\phi_i + v_i - \bar{\phi}_i)(\phi_i - 1). \quad (56)$$

Define $\dot{k}_M$ as the upper bound of $\dot{\mathcal{K}}(t)$. Then

$$\frac{1}{2}\sum_{i=1}^{N} \dot{k}_i(2\phi_i + v_i)v_i$$
$$\leq \frac{\dot{\mathcal{K}}_M}{\mathcal{K}_m\lambda_{\min}(P)}\vartheta^T[\mathcal{K}(t)(\phi + v) \otimes PP]\vartheta. \quad (57)$$

It follows from (48)−(57) that (49) satisfies:

$$\dot{V} = \dot{V}_1 + \dot{V}_2$$
$$\leq 2\eta^T\Gamma\mathcal{A}\eta + (\chi_1^{-1} + \chi_2^{-1}c)\eta^T\Gamma\Gamma\eta + \chi_1\beta^T\beta$$
$$+ \chi_3^{-1}\eta^T\Gamma\mathcal{B}\mathcal{B}^T\Gamma\eta$$
$$+ \sum_{i=1}^{N}\alpha_i^T(\chi_4^{-1}\mathcal{M}\mathcal{M}^T + \chi_{11}^{-1}C^T L^T LC)\alpha_i$$
$$+ \sum_{i=1}^{N}\tilde{h}_i^T(\chi_5^{-1}\mathcal{U}\mathcal{U}^T + \chi_{12}^{-1}L^T L)\tilde{h}_i$$
$$+ \sum_{i=1}^{N}[\frac{(\chi_4 + \chi_5)\chi_6}{2}\varphi_{mi}^4 + 4\chi_3\varphi_{mi}^2 + \chi_{10}^{-1} + \frac{\chi_7}{2}k_{\hat{W}_i}]\check{W}_i^2$$
$$- \sum_{i=1}^{N}[(1 - \frac{1}{2\chi_7})k_{\hat{W}_i} - \frac{(\chi_4 + \chi_5)}{2\chi_6} - \chi_9^{-1}]\|\tilde{W}_i\|_F^2 \quad (58)$$

$$+ \vartheta^T (\phi + \upsilon) \mathcal{K}(t) \otimes \{PA + A^T P + \varsigma PP\} \vartheta$$

$$- \sum_{i=1}^{N} \{[c\lambda_0 - ((\chi_9 \varphi_{mi}^2 + \chi_{10}) \|B^T\|^2 + (\chi_{11} + \chi_{12})) \lambda_\Xi$$

$$- \chi_2 c \|I_2 - BB^T\|^2](\phi_i + \upsilon_i)^2 + s_i \bar{\phi}_i k_i\} \|P\vartheta_i\|^2$$

$$+ \sum_{i=1}^{N} \frac{\nu_{\phi_i} k_i}{4} (\phi_i - 1)^2 - \sum_{i=1}^{N} k_i \nu_{\phi_i} (\phi_i + \upsilon_i - \bar{\phi}_i)(\phi_i - 1)$$

$$\tag{59}$$

where $\varsigma = s_i + \frac{\chi_8 + \chi_8^{-1} \lambda_{\max}(\dot{\mathcal{L}}_1^T(t) \dot{\mathcal{L}}_1(t)) \|\mathcal{L}_1^{-1}(t)\|^2 + \check{\mathcal{K}}_M}{\check{\mathcal{K}}_m \lambda_{\min}(P)}$. Sufficiently small χ_9, χ_{10}, χ_{11}, χ_{12}, χ_2 such that $\varrho = c\lambda_0 - ((\chi_9 \varphi_{mi}^2 + \chi_{10}) \|B^T\|^2 + (\chi_{11} + \chi_{12})) \lambda_\Xi - \chi_2 c \|I_2 - BB^T\|^2 > 0$ and $(1 - \frac{1}{2\chi_7}) k_{\hat{W}_i} - \frac{(\chi_4 + \chi_5)}{2\chi_6} - \chi_9^{-1} \geq \epsilon_i$ hold. ϵ_i is a positive constant. Moreover, a sufficiently large $\bar{\phi}_i > 0$ can ensure that $\bar{\phi}_i > \max\left\{\frac{1 + \varsigma + s_i^2 \mathcal{K}_m^2}{4\varrho s_i k_i}, \frac{1}{\beta_i k_i \varpi_2}, \frac{1}{\beta_i}, \frac{1}{\beta_i k_i \varpi_1}, \frac{\mathcal{W}_{2i}}{\beta_i}, \frac{\mathcal{W}_{2i}}{\beta_i}\right\}$ holds.

Note that

$$-(\phi_i - 1)(\phi_i - \bar{\phi}_i) = -(\phi_i - \bar{\phi}_i)^2 - (\bar{\phi}_i - 1)(\phi_i - \bar{\phi}_i)$$

$$\leq -\frac{1}{2}(\phi_i - \bar{\phi}_i)^2 + \frac{1}{2}(\bar{\phi}_i - 1)^2 \tag{60}$$

and

$$-(\phi_i - 1)(\phi_i - \bar{\phi}_i) = -(\phi_i - 1)^2 - (\bar{\phi}_i - 1)(\phi_i - \bar{\phi}_i)$$

$$\leq -\frac{1}{2}(\phi_i - 1)^2 + \frac{1}{2}(\bar{\phi}_i - 1)^2. \tag{61}$$

Furthermore,

$$- \sum_{i=1}^{N} k_i \nu_{\phi_i} (\phi_i - \bar{\phi}_i)(\phi_i - 1)$$

$$= \sum_{i=1}^{N} \frac{k_i \nu_{\phi_i}}{2} (\bar{\phi}_i - 1)^2$$

$$- \frac{k_i \nu_{\phi_i}}{4} [(\phi_i - \bar{\phi}_i)^2 + (\phi_i - 1)^2]. \tag{62}$$

Then,

$$\dot{V} \leq -\delta V - \vartheta^T ((\phi + \upsilon) \mathcal{K}(t) \otimes (I_N - \delta P)) \vartheta$$

$$- \eta^T (\mathcal{V} - \delta \Gamma) \eta - \sum_{i=1}^{N} \left(\frac{\nu_{\phi_i} k_i}{4} - \frac{\delta s_i}{2}\right)(\phi_i - \bar{\phi}_i)^2$$

$$- \sum_{i=1}^{N} \left(\epsilon_i - \frac{\delta}{2\Gamma_{W_i}}\right) \|\tilde{W}_i\|_F^2 + \Xi \tag{63}$$

where

$$\Xi = \sum_{i=1}^{N} \left[\frac{(\chi_4 + \chi_5)\chi_6 + 8\chi_3 + 2\chi_{10}^{-1}}{2} \varphi_m^2 + \frac{\chi_7}{2} k_{\hat{W}_i}\right] \check{W}_i^2$$

$$+ \frac{1}{2} \sum_{i=1}^{N} k_i \nu_{\phi_i} (\bar{\phi}_i - 1)^2 + \chi_1 \sum_{i=1}^{N} (\check{\varepsilon}_i^2 + \bar{h}_i^2). \tag{64}$$

Moreover, based on the condition $0 < \delta \leq \min_{i=1,2,\ldots,N} \times \left\{\frac{\nu_{\phi_i} k_i}{2s_i}, \frac{1}{2\lambda_{\max}(P)}, \frac{1}{2\lambda_{\max}(\Gamma)}, 2\epsilon_i \Gamma_{W_i}\right\}$, (59) satisfies the following inequality:

$$\dot{V} \leq -\delta V + \Xi. \tag{65}$$

Therefore η, $\tilde{W}$, ϑ, ϕ and ϑ can converge exponentially to the following bounded set:

$$\mathcal{D} \triangleq \left\{\eta, \tilde{W}, \vartheta, \phi : V \leq \frac{1}{\delta} \Xi\right\}. \tag{66}$$

                                                    ∎

Remark 5: In this paper, communication faults parameters are usually time-varying. When using the Lyapunov method, the derivatives of the parameters associated with the Laplace matrix must be introduced. Therefore, matrix B is not required in the observer controller $\hat{u}_i$ and its adaptive rate ϕ_i design.

Remark 6: Designing adaptive output feedback tracking protocols is more challenging due to the asymmetric Laplacian matrix of the directed graph. The adaptive gain ϕ_i is used to estimate the eigenvalue information of the asymmetric Laplacian matrix associated with the directed graph. If the existing methods in [27] and [31] are used, the adaptive parameter ϕ_i is updated by $\phi_i = \vartheta_i^T(t) PBB^T P\vartheta_i(t)$. It is easy to see the parameter ϕ_i will increase monotonically. To avoid this phenomenon, a σ-modification technique is introduced in (20).

Remark 7: We introduce dynamic coupling gains ϕ_i and υ_i to avoid global information and information related to the fault parameters. These gains are updated in dependence on the relative error $\vartheta_i(t)$.

V. SIMULATION RESULTS

This section aims to demonstrate the feasibility and effectiveness of the proposed resilient PCC voltage regulation strategy based on containment and output feedback and the resilience of the strategy under communication faults and sensor faults. For this purpose, we have simulated in the MATLAB/Simulink software environment for the MG shown in Fig. 3. The MMS is tested with a combination of four sub-MGs. For simplicity, each sub-MG consists of only one DG. Table I provides the parameters of DGs, lines and loads in Fig. 3. It is assumed that the DGs communicate with each other through the directed topology shown in Fig. 4. DG#1, DG#4 receive information from v_{ref1}, v_{ref2}, respectively. Then, after calculation, it is possible to obtain $\bar{x} = \text{col}\{222.8571, 211.4286, 228.5714, 234.2857\}$.

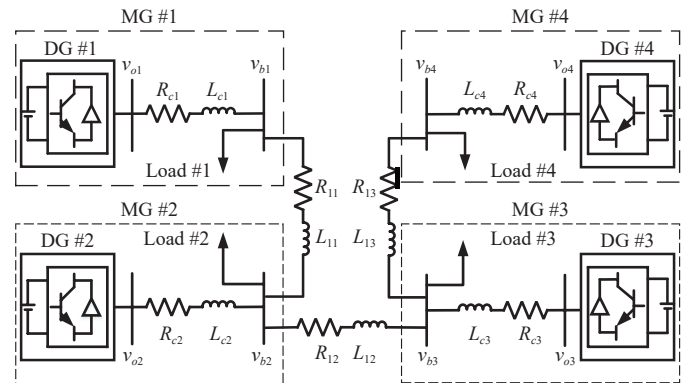This case scenario examines the capability of the proposed

Fig. 3.   The example MG test system.

TABLE I
SPECIFICATIONS OF THE MG TEST SYSTEM

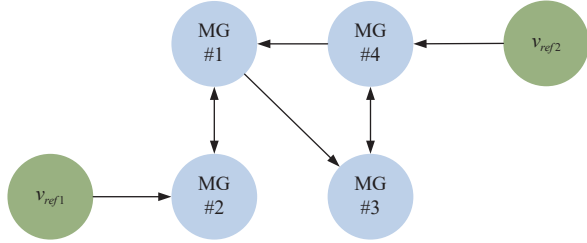| DGs	DG#1 & DG#2 & DG#3 & DG#4		
m_P	1.5×10^{-5}		
n_Q	2×10^{-4}		
Lines	$R_{l1} = R_{l3} = 1 \times 10^{-4} \ \Omega$		$R_{l2} = 1 \times 10^{-4} \ \Omega$
	$L_{l1} = L_{l3} = 3.18 \times 10^{-4} \ \text{mH}$		$L_{l2} = 1.847 \ \text{mH}$
RL loads	Load #1 & Load #4	Load #2	Load #3
P (per phase)	12 kW	100 kW	20 kW
Q (per phase)	12 kVAr	24 kVAr	10 kVAr

Fig. 4.   The considered communication structure.

resilient voltage regulation approach after islanding at $t = 0.0$ s. For this purpose, the following four test scenarios were performed:

1) At $t = 0.4$ s, the containment-based PCC voltage regulation secondary control cuts in.

2) At $t = 0.7$ s, MG #4 was disconnected.

3) At $t = 1$ s, MG #4 was reconnected.

4) At $t = 1.3$ s, load #1 cuts off 50%.

5) At $t = 1.6$ s, 50% of load #1 is restored to its original value.

Solving (33) gives a solution

$$P = \begin{bmatrix} 0.9102 & 0.4142 \\ 0.4142 & 1.2872 \end{bmatrix}.$$

We define $v_{ref1} = 200$, $v_{ref2} = 240$. We choose the control parameters of the containment-based PCC algorithm as $c = 1.5E + 7$, $\nu_{\phi_i} = 1$, $\iota_{y_i} = 5$, $\Gamma_{\hat{W}_i} = \iota_{\hat{W}_i} = 1$, $k_{\hat{W}_i} = 30$, and $i = 1, 2, \ldots, 4$. Let $\phi_i(0.4) = 1$ and $\hat{W}_i(0.4) = 1$ be the initial values of $\phi_i(t)$ and $\hat{W}_i(t)$, $i = 1, 2, \ldots, N$, respectively. The communication links faults are chosen as: $\delta_{12}^a = 0.5\sin(t)$, $\delta_{14}^a = 0.5\sin(t)$, $\delta_{25}^a = 0.1\sin(t)$, $\delta_{21}^a = 0.5\sin(t)$, $\delta_{32}^a = 0.5\cos(t)$, $\delta_{34}^a = 0.5\sin(t)$, $\delta_{43}^a = 0.5\cos(t)$, $\delta_{46}^a = 0.1\cos(t)$. The sensors faults are chosen as: $h_1 = 0.5\cos(t + 10) + 0.1$, $h_2 = 0.8$, $h_3 = 0.8\cos(6t + 3) + 0.1$, $h_4 = 0.9$.

To verify the effectiveness of the containment-based PCC regulation algorithm in an MMS, the algorithm initially relies on only primary control to maintain voltage stability by adjusting the droop factor. As shown in Fig. 5, the primary control successfully achieves voltage stability and provides a timely response. However, operation in differential mode causes the voltage to deviate from the nominal value. Therefore, introducing a designed regulation control layer is crucial for the cooperative regulation of PCC voltages in an MMS. After the secondary control algorithm is activated when $t = 0.4$ s, it is observed that the PCC voltages are regulated
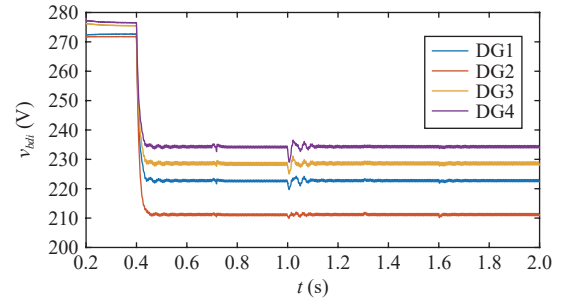
Fig. 5.   The PCC voltages v_{bdi}^*, $i = 1, 2, \ldots, 4$.

into a convex packet formed by reference values v_{ref1}, v_{ref2}, thus, the voltage is restored within a reasonable range while a voltage difference exists between the PCC voltages to achieve the power flow between the MGs. At $t = 0.7$ s and $t = 1.0$ s, the PCC voltages fluctuate due to the separation and subsequent reconnection of the sub-MGs. The voltage quickly returns to its original value, indicating that the regulation strategy effectively maintains voltage stability. Similarly, at $t = 1.3$ s and $t = 1.6$ s, the proposed PCC voltage regulation strategy effectively restores the desired voltage level after the load is temporarily disconnected and converted. In addition, Figs. 6−9 indicate the corresponding output voltage, controller, and active and reactive power changes, further illustrating the effectiveness of the voltage regulation proposed in this paper.
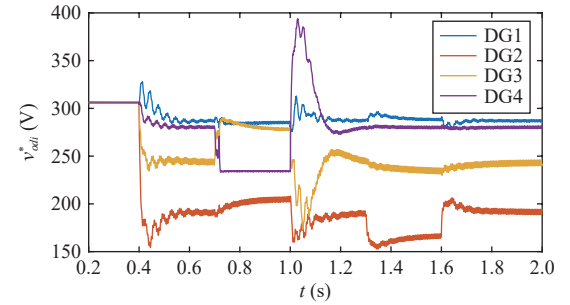
Fig. 6.   Output terminal voltage v_{odi}^*, $i = 1, 2, \ldots, 4$.
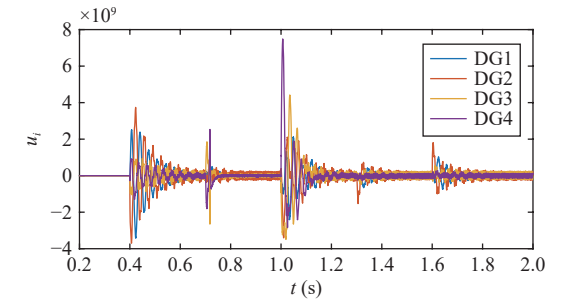
Fig. 7.   The controllers u_i, $i = 1, 2, \ldots, 4$.

In summary, the effectiveness of the containment-based PCC voltage regulation strategy proposed in this study is verified under load shifting and plugging scenarios, providing a reliable means to ensure the stable operation of the MG system.
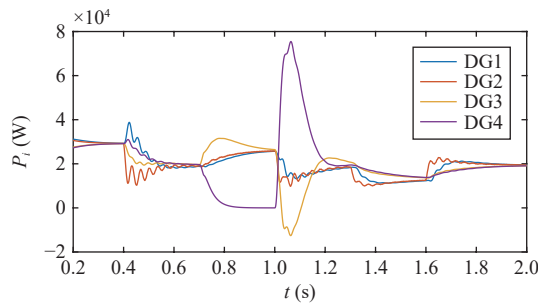
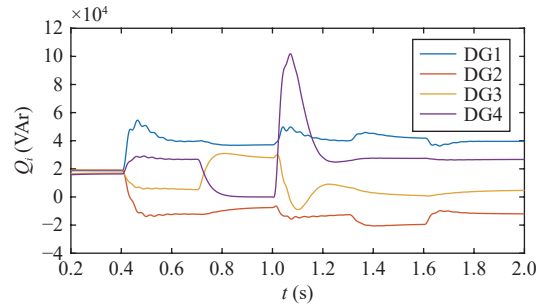Fig. 8. The active power P_i, $i = 1, 2, \ldots, 4$.

Fig. 9. The reactive power Q_i, $i = 1, 2, \ldots, 4$.

VI. CONCLUSIONS

This paper has proposed a containment-based AC MG secondary control strategy to regulate the PCC voltage. Unlike previous voltage regulation strategies, the applied feedback linearization transforms the PCC voltage regulation control into a distributed output feedback tracking problem of a linear MAS with nonlinear dynamics. If multiple PCC voltages are set to return to the reference voltage collectively, it will not be possible to perform power flow between sub-MGs. Therefore, the idea of containment control is introduced. The control objective is to restore to a reasonable range while there is a voltage difference between PCC voltages. In addition, network communication between DGs and sensor failures in DGs are unavoidable. A novel resilient fault-tolerant control algorithm with output feedback based on state observer has proposed to achieve communication resilience while avoiding the effects of sensor failures. At the same time, it avoids the global information of the directed communication network and fault parameters related to applications.

REFERENCES

[1] R. Wang, Q. Sun, P. Zhang, Y. Guo, D. Qin, and P. Wang, "Reduced-order transfer function model of the droop-controlled inverter via Jordan continued-fraction expansion," *IEEE Trans. Energy Convers.*, vol. 35, no. 3, pp. 1585–1595, Sept. 2020.

[2] Q. Sun, B. Wang, X. Feng, and S. Hu, "Small-signal stability and robustness analysis for microgrids under time-constrained DoS attack and a mitigation adaptive secondary control method," *Sci. China Inf. Sci.*, vol. 65, p. 162202, 2022.

[3] T. Qian, Y. Liu, W. Zhang, W. Tang, and M. Shahidehpour, "Event-triggered updating method in centralized and distributed secondary controls for islanded microgrid restoration," *IEEE Trans. Smart Grid*, vol. 11, no. 2, pp. 1387–1395, Mar. 2020.

[4] W. Gu, G. Lou, W. Tan, and X. Yuan, "A nonlinear state estimator-based decentralized secondary voltage control scheme for autonomous microgrids," *IEEE Trans. Power Syst.*, vol. 32, no. 6, pp. 4794–4804, Nov. 2017.

[5] B. Fan, J. Peng, J. Duan, Q. Yang, and W. Liu, "Distributed control of multiple-bus microgrid with paralleled distributed generators," *IEEE/CAA J. Autom. Sinica*, vol. 6, no. 3, pp. 676–684, May 2019.

[6] Z. Li, C. Zang, P. Zeng, H. Yu, and H. Li, "MAS based distributed automatic generation control for cyber-physical microgrid system," *IEEE/CAA J. Autom. Sinica*, vol. 3, no. 1, pp. 78–89, Jan. 2016.

[7] X. Li, Z. Sun, Y. Tang, and H. R. Karimi, "Adaptive event-triggered consensus of multiagent systems on directed graphs," *IEEE Trans. Autom. Control*, vol. 66, no. 4, pp. 1670–1685, Apr. 2021.

[8] Z. Li, W. Ren, X. Liu, and M. Fu, "Consensus of multi-agent systems with general linear and Lipschitz nonlinear dynamics using distributed adaptive protocols," *IEEE Trans. Autom. Control*, vol. 58, no. 7, pp. 1786–1791, Jul. 2013.

[9] S. Liu, J. Sun, H. Zhang, and M. Zhai, "Fully Distributed event-driven adaptive consensus of unknown linear systems," *IEEE Trans. Neural Netw. Learn. Syst.*, 2022. DOI: 10.1109/TNNLS.2022.3148824.

[10] B. Ning, Q. L. Han, Z. Zuo, L. Ding, Q. Lu, and X. Ge, "Fixed-time and prescribed-time consensus control of multiagent systems and its applications: A survey of recent trends and methodologies," *IEEE Trans. Ind. Informat.*, vol. 19, no. 2, pp. 1121–1135, Feb. 2023.

[11] W. S. Im, C. Wang, W. Liu, L. Liu, and J.-M. Kim, "Distributed virtual inertia based control of multiple photovoltaic systems in autonomous microgrid," *IEEE/CAA J. Autom. Sinicaa*, vol. 4, no. 3, pp. 512–519, 2017.

[12] J. Hu, Q. Sun, R. Wang, B. Wang, M. Zhai, and H. Zhang, "Privacy-preserving sliding mode control for voltage restoration of AC microgrids based on output mask approach," *IEEE Trans. Ind. Informat.*, vol. 18, no. 10, pp. 6818–6827, Oct. 2022.

[13] A. Bidram, A. Davoudi, F. L. Lewis, and J. M. Guerrero, "Distributed cooperative secondary control of microgrids using feedback linearization," *IEEE Trans. Power Syst.*, vol. 28, no. 3, pp. 3462–3470, Aug. 2013.

[14] J. Zhou, S. Kim, H. Zhang, Q. Sun, and R. Han, "Consensus-based distributed control for accurate reactive, harmonic, and imbalance power sharing in microgrids," *IEEE Trans. Smart Grid*, vol. 9, no. 4, pp. 2453–2467, Jul. 2018.

[15] N. M. Dehkordi, N. Sadati, and M. Hamzeh, "Distributed robust finite-time secondary voltage and frequency control of islanded microgrids," *IEEE Trans. Power Syst.*, vol. 32, no. 5, pp. 3648–3659, Sept. 2017.

[16] B. Ning, Q.-L. Han, and L. Ding, "Distributed secondary control of AC microgrids with external disturbances and directed communication topologies: A full-order sliding-mode approach," *IEEE/CAA J. Autom. Sinica*, vol. 8, no. 3, pp. 554–564, Mar. 2021.

[17] M. Zhai, Q. Sun, B. Wang, Z. Liu, and H. Zhang, "Cooperative fault-estimation-based event-triggered fault-tolerant voltage restoration in islanded AC microgrids," *IEEE Trans. Autom. Sci. Eng.*, vol. 20, no. 3, pp. 1829–1837, Jul. 2023.

[18] C. Deng and W.-W. Che, "Fault-tolerant fuzzy formation control for a class of nonlinear multiagent systems under directed and switching topology," *IEEE Trans. Syst., Man, Cybern., Syst.*, vol. 51, no. 9, pp. 5456–5465, Sept. 2021.

[19] J. Sun, Z. Tan, S. Liu, H. Zhang, and W. Chuo, "Fully distributed event-driven coordination with actuator faults," *IEEE Trans. Cybern.*, 2022. DOI: 10.1109/TCYB.2022.3198499

[20] A. Afshari, M. Karrari, H. R. Baghaee, G. B. Gharehpetian, and S. Karrari, "Cooperative fault-tolerant control of microgrids under switching communication topology," *IEEE Trans. Smart Grid*, vol. 11, no. 3, pp. 1866–1879, May 2020.

[21] A. Afshari, M. N. Karrari, H. R. Baghaee, and G. B. Gharehpetian, "Distributed fault-tolerant voltage/frequency synchronization in autonomous AC microgrids," *IEEE Trans. Power Syst.*, vol. 35, no. 5, pp. 3774–3789, Sept. 2020.

[22] M. Zhai, Q. Sun, R. Wang, B. Wang, S. Liu, and H. Zhang, "Fully distributed fault-tolerant event-triggered control of microgrids under directed graphs," *IEEE Trans. Netw. Sci. Eng.*, vol. 9, no. 5, pp. 3570–3579, 2022.

[23] M. Zhai, Q. Sun, R. Wang, B. Wang, J. Hu, and H. Zhang, "Distributed multiagent-based event-driven fault-tolerant control of islanded microgrids," *IEEE Trans. Cybern.*, 2023. DOI: 10.1109/TCYB.2023.3266923.

[24] X. Li, C. Wen, C. Chen, and Q. Xu, "Adaptive resilient secondary control for microgrids with communication faults," *IEEE Trans. Cybern.*, vol. 52, no. 8, pp. 8493–8503, Aug. 2022.

[25] S. Abhinav, I. D. Schizas, F. Ferrese, and A. Davoudi, "Optimization-based AC microgrid synchronization," *IEEE Trans. Ind. Informat.*, vol. 13, no. 5, pp. 2339–2349, Oct. 2017.

[26] Y. Wang, T. L. Nguyen, M. H. Syed, Y. Xu, E. Guillo-Sansano, V. H. Nguyen, G. M. Burt, Q. T. Tran, and R. Caire, "A distributed control scheme of microgrids in energy internet paradigm and its multisite implementation," *IEEE Trans. Ind. Informat.*, vol. 17, no. 2, pp. 1141–1153, Feb. 2021.

[27] N. M. Dehkordi, H. R. Baghaee, N. Sadati, and J. M. Guerrero, "Distributed noise-resilient secondary voltage and frequency control for islanded microgrids," *IEEE Trans. Smart Grid*, vol. 10, no. 4, pp. 3780–3790, Jul. 2019.

[28] B. Ning, Q.-L. Han, and L. Ding, "Distributed finite-time secondary frequency and voltage control for islanded microgrids with communication delays and switching topologies," *IEEE Trans. Cybern.*, vol. 51, no. 8, pp. 3988–3999, Aug. 2021.

[29] C. Deng, F. Guo, C. Wen, D. Yue, and Y. Wang, "Distributed resilient secondary control for DC microgrids against heterogeneous communication delays and DoS attacks," *IEEE Trans. Ind. Electron.*, vol. 69, no. 11, pp. 11560–11568, Nov. 2022.

[30] C. Chen, K. Xie, F. Lewis, S. Xie, and R. Fierro, "Adaptive synchronization of multi-agent systems with resilience to communication link faults," *Automatica*, vol. 111, p. 108636, Jan. 2020.

[31] J. Zhang and H. Zhang, "Adaptive event-triggered consensus of linear multiagent systems with resilience to communication link faults for digraphs," *IEEE Trans. Circuits Syst. II*, *Exp. Briefs*, vol. 69, no. 7, pp. 3249–3253, Jul. 2022.

[32] Z. Peng, D. Wang, H. Zhang, and G. Sun, "Distributed neural network control for adaptive synchronization of uncertain dynamical multiagent systems," *IEEE Trans. Neural Netw. Learn. Syst.*, vol. 25, no. 8, pp. 1508–1519, Aug. 2014.

Meina Zhai received the B.S. degree in mathematics and applied mathematics from Shenyang Normal University in 2016, the M.S. degree in systems analysis and integration from Northeastern University in 2019. She is currently a Ph.D. candidate in control science and engineering, Northeastern University.

Her research interests include microgrids, voltage regulation, fault-tolerant control, event-triggered control and adaptive control.

Qiuye Sun (Senior Member, IEEE) received the Ph.D. degree in control theory and control engineering from Northeastern University in 2007. He is currently a Full Professor with Northeastern University and obtained Special Government Allowances from the State Council in China. His current research interests include optimization analysis technology of power distribution network, network control of energy Internet, integrated energy systems and microgrids.

He has authored or coauthored over 200 papers, authorized over 100 invention patents, and published over 10 books or textbooks. He is an Associate Editor of *IEEE Trans NNLS*, *IET Cyber-Physical Systems*, *CSEE Journal of Power and Energy Systems*, *IEEE/CAA Journal of Automatica Sinica*, etc.

Rui Wang received the B.S. degree in electrical engineering and automation and the Ph.D. degree in power electronics and power drive from Northeastern University, in 2016 and 2021, respectively. In 2019, he became a Visiting Scholar with the Energy Research Institute, Nanyang Technological University, Singapore. He is a Lecturer with Northeastern University. His research interest focuses on collaborative optimization of distributed generation and its stability analysis in cyber-energy system.

He has authored or coauthored over 50 papers, authorized over 20 invention patents. As the first author, he obtained IEEE Transactions on Energy Conversion Best Paper Award in 2021. He is an Editor or Guest Editor of *Frontiers in Energy Research*, *Wireless Power Transfer*.

Huaguang Zhang (Follow, IEEE) received the B.S. and M.S. degrees in control engineering from the Northeast Dianli University, in 1982 and 1985, respectively, and the Ph.D. degree in thermal power engineering and automation from Southeast University in 1991. He joined the Department of Automatic Control, Northeastern University in 1992, as a Post-Doctoral Fellow for two years. Since 1994, he has been a Professor and the Head of the School of Information Science and Engineering, Institute of Electric Automation, Northeastern University. His current research interests include fuzzy control, stochastic system control, neural networks based control, nonlinear control, and their applications.

Dr. Zhang has authored or co-authored over 280 journal and conference papers and six monographs and co-invented 90 patents. He was a recipient of the Outstanding Youth Science Foundation Award from the National Natural Science Foundation Committee of China in 2003. He was named the Cheung Kong Scholar by the Education Ministry of China in 2005. He was also a recipient of the IEEE Transactions on Neural Networks 2012 Outstanding Paper Award and the Andrew P. Sage Best Transactions Paper Award 2015. He is the E-Letter Chair of the IEEE CIS Society and the former Chair of the Adaptive Dynamic Programming & Reinforcement Learning Technical Committee on the IEEE Computational Intelligence Society. He was an Associate Editor of the *IEEE Transactions on Fuzzy Systems* from 2008 to 2013. He is an Associate Editor of *Automatica*, the IEEE *Transactions on Neural Networks* and *Learning Systems*, the *IEEE Transactions on Cybernetics*, and *Neurocomputing*.